Performance of multi-code CDMA in a multipath fading channel

D.-W.Hsiung and J.-F.Chang

Abstract: The authors provide a general investigation on the performance of multi-code code division multiple access (MC-CDMA) over Rayleigh fading plus additive white Gaussian noise (AWGN) channels. In MC-CDMA, high speed data sources are serial-to-parallel converted to low speed streams, which are further spread by Hadamard–Walsh orthogonal sequences and random codes. Numerical results show that, in a multipath fading channel, MC-CDMA with properly assigned Hadamard–Walsh sequences outperforms conventional CDMA when signal to noise ratio (SNR) is low and shows comparable performance at high SNR. Furthermore, for the AWGN channel, the approximate formula developed by Lee *et al.* (1997) shows more variation than the authors' formula. The new approach is capable of telling the impact of code cross-correlation on system performance while the earlier approach does not.

1 Introduction

In recent few years, a new form of code division multiple access (CDMA) known as multi-code code division multiple access (MC-CDMA) has induced considerable research interests in multirate transmission [1, 2]. MC-CDMA, a wireless framework, has appealing features in supporting multimedia (e.g. data, voice, image, and video). The number of codes allocated by a central control unit (e.g. base station) is linearly proportional to a user's rate. To realise this idea, high speed traffic sources are serial-to-parallel converted to low speed streams, each occupying the same bandwidth. MC-CDMA inherits the strength of CDMA in combating multipath fading and requires no need to modify the radio frequency circuitry [1, 3]. Furthermore, interchip interference (ICI) and intersymbol interference (ISI) are mitigated due to the usage of subcode concatenation [3] among all parallel streams. After demodulation, maximal ratio combining (MRC) [4] is performed in the correlation receivers in order to reconstruct the original source bits.

Lately, focus has concentrated on the performance including system capacity of direct sequence CDMA (DS-CDMA) scheme in a variety of channel models. [5, 6] offer the analysis of DS-CDMA in an AWGN channel and Rician fading channel, respectively. The fundamental concept is to regard every user except the intended one as an interferer and model it as uncorrelated Gaussian noise. A glance at the conception can also be found in the papers (e.g. [7–9]). Besides, code design is a primary cause affecting the performance of variable rate CDMA. [10, 11] present the impact of code design on the performance of multirate CDMA. However, in the analysis an AWGN channel is assumed that makes the results only approximate. [12] reports the capacity of a DS-CDMA system that supports various quality of services (QoSs). However, the analytical results stated in the works (e.g. [12–15]), are not satisfactory. These results do not reveal the impact of code assignment on system performance. That is, different primary codes and orthogonal subcodes show unnoticeable difference in (e.g. BER and capacity). A more precise performance comparison between conventional CDMA and MC-CDMA in various channel models is highly helpful in demonstrating the strength of MC-CDMA. The objective of this paper is to offer a more comprehensive analysis of MC-CDMA in a frequency selective fading channel. The analysis developed in this paper is a generalisation of [12, 5]; but, the problem treated is extended to include the multipath fading channel.

In this paper, we derive the bit error rate of MC-CDMA with higher accuracy. The result shows that MC-CDMA outperforms conventional CDMA, especially in delay non-sensitive applications. Furthermore, the approximate formula developed in [12] over an AWGN channel shows considerably more variation than ours.

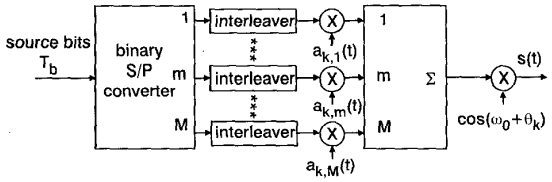

Fig. 1 *Multi-code CDMA transmitter of user k*

2 System model

2.1 Transmitter-receiver pair and code assignment

The transmitter and receiver pair are shown, respectively, in Figs. 1 and 3. Fig. 2 shows the main lobe spectrum of the transmitted signal. For simplicity, forward error correction (FEC) is not considered. On the transmitting side, assume there are K users in the multi-code system, each transmitting at rates corresponding to code numbers M_1, ..., M_k, ...,

IEE Proceedings online no. 20000686

DOI: 10.1049/ip-com.20000686

Paper first received 2nd April 1999 and in revised form 30th May 2000

The authors are with the Department of Electrical Engineering and the Graduate Institute of Communication Engineering, National Taiwan University, Taipei, Taiwan 10764, Republic of China

M_K, respectively. Let M denote the code number corresponding to full rate, then ($1 \le M_k \le M$). That is, for the kth user ($1 \le k \le K$), its bit stream with duration $T_b^{[k]}$ is serial-to-parallel converted to M_k parallel streams. The new bit duration becomes $T = M_k T_b^{[k]}$. Each bit is further spread by a sequence with processing gain N. The bits in each stream are interleaved to break correlated channel errors caused by (e.g.) a multipath channel. To make the problem simple, the interleavers and the de-interleavers are not shown in Figs. 1 and 3. The chip duration T_c of each concatenated subcode $a_{k,m}(t)$ for the mth stream can be found to be

$$T_c = \frac{M_k}{N} T_b^{[k]} \tag{1}$$

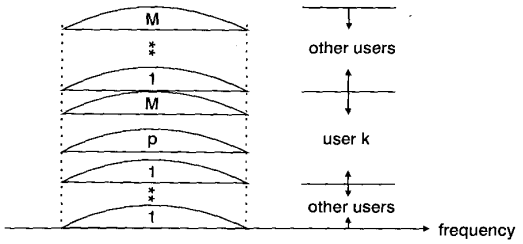

Fig. 2 *Main lobe spectrum of transmitted signal*

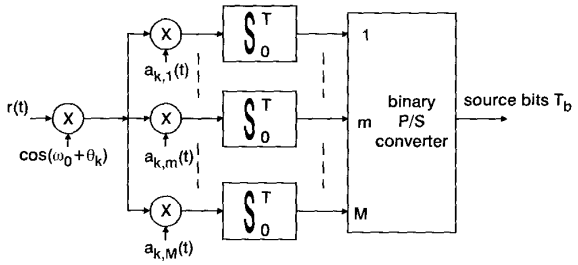

Fig. 3 *Multi-code CDMA receiver of user k with MF for each code*

Each user admitted to the system is assigned a primary code and a specific row of the Hadamard–Walsh matrix by a central control unit. The primary codes of different users are random codes which are only approximately orthogonal. To avoid self-interference, mutually orthogonal subcodes are created by multiplying the primary code and the rows of Hadamard–Walsh matrix bitwise. This is known as subcode concatenation technique in [2]. The rows of Hadamard–Walsh matrix shared by users should be arranged so as to avoid if possible the same row being used by different users. For example, if there are ten users in the system and we use the Hadamard–Walsh matrix of dimension 64, $\lfloor 64/10 \rfloor = 6$ where $\lfloor x \rfloor$ denotes the largest integer less than x. If the first user starts with the 1st row, the kth user is suggested to start at the $(k-1)6 + 1$st row. Define $\hat{M} = \lfloor N/K \rfloor$. What is meant in this example is that user 1 uses rows 1, 2, ..., M_1, while user k uses rows $(k-1)6 + 1$, $(k-1)6 + 2$, ..., $(k-1)6 + M_k$ as their subcodes. This code assignment scheme can accommodate the greatest number of mutually orthogonal subcodes for a given number of users. For convenience, we number the mth subcode of the kth user by $(k-1)\hat{M} + m$, and the corresponding subcode may further be represented as

$$a_{k,m}(t) = \sum_{j=-\infty}^{\infty} a^{[j]}_{(k-1)\hat{M}+m} \Pi_{T_c}(t - jT_c) \tag{2}$$

where $\Pi_{T_c}(t)$ is the unit gate function with height 1 when $0 \le t \le T_c$, and 0 otherwise. In eqn. 2, $a^{[j]}_{(k-1)\hat{M}+m}$ represents the jth bit of the sequence $a_{k,m}(t)$. Further discussions about the primary codes are presented in Section 4.

Without loss of generality and to comply with the orthogonality condition of Hadamard sequences, the binary elements in this paper are represented by +1 and –1 using the mapping $1 \rightarrow -1$ and $0 \rightarrow +1$. The signal transmitted from user k is

$$s_k(t) = \sum_{m=1}^{M_k} \sqrt{2P} b_{k,m}(t) a_{k,m}(t) \cos(\omega_0 t + \theta_k) \tag{3}$$

where $b_{k,m}(t)$ denotes the bit series fed from the mth stream. Also in eqn. 3, P is the signal power, ω_0 is the carrier frequency, and θ_k is a random phase uniformly distributed on $[0, 2\pi)$. The θ_ks are independent and identically distributed (i.i.d.) for all users.

The receiver of user k sketched in Fig. 3 utilises M_k RAKE receivers for the M_k parallel streams prior to the de-interleavers and threshold devices. The RAKE receiver performs maximal ratio combining and post-detection to reconstruct the original bit stream. It is believed that no change is needed in the IF/RF circuitry except for the control and adjustment of transmission power to meet different source rates and QoS objectives Fig. 1.

2.2 Channel model

A variety of channel models have been proposed and used in different transmission environments [4, 7, 16]. In this paper the channel is assumed to be slowly varying Rayleigh fading with a continuum of multipaths. The impulse response of the channel carrying L paths can be described as

$$c_k(t) = \sum_{l=1}^{L} g_{k,l} \delta(t - t_{k,l}) \tag{4}$$

where $g_{k,l} = \alpha_{k,l} e^{j\phi_{k,l}}$ is a complex Gaussian random variable (r.v.) with zero mean and $\alpha_{k,l}$ is Rayleigh distributed with variance σ_l^2. In eqn. 4, $t_{k,l} = (l-1)T_c + \delta_{k,l}$ is the delay of the lth of the kth user. Random variables $\delta_{k,l}$ and $\phi_{k,l}$ are uniformly distributed on $[0, T_c]$ and $[0, 2\pi)$, respectively. Owing to perfect power control assumption among the MC CDMA users, $\alpha_{k,l}$, $\phi_{k,l}$, as well as $\delta_{k,l}$ can be viewed as i.i.d. for all k and l.

The channel autocovariance function defined in [4] can be easily found to be

$$\mu_k(t) = \sum_{l=1}^{L} \sigma_l^2 \delta(t - t_{k,l}) \tag{5}$$

In this paper, we assume equal power delay profile for all paths (i.e. any path locked by the RAKE receiver is with equal power). There is no influence on the result in which one or more of the paths are locked by the matched filters (MFs). Notice that the spreading codes obtained by subcode concatenation have an impact on the BER that relies on the power delay profile of the channel. This impact can be ignored only for perfectly 'random codes'.

3 Analysis

It is assumed that perfect chip, symbol, and carrier synchronisation are performed in the system. The received power per user stream is equal to P, if no fading effect is concerned. For convenience and yet no loss of generality, user 1 is assumed to be the intended receiver in the following discussions. The signal received by user 1 in a K-user system can be written as follows:

$$r(t) = n(t) + \sqrt{2P}\sum_{k=1}^{K}\sum_{m=1}^{M_k}\sum_{l=1}^{L}\alpha_{k,l}b_{k,m}(t-t_{k,l}-\tau_k) \times a_{k,m}(t-t_{k,l}-\tau_k)\cos(\omega_0 t+\zeta_{k,l}) \quad (6)$$

where $n(t)$ is AWGN with zero mean and double-sided power spectral density (p.s.d.) $N_0/2$, τ_k is the propagation delay of user k, and $\zeta_{k,l} = (\theta_k + \phi_{k,l} - \omega_0 t_{k,l} - \omega_0\tau_k) \bmod 2\pi$. Random variables τ_k and $\zeta_{k,l}$ are both uniformly distributed on $[0, T)$ and $[0, 2\pi)$, respectively. Notice that, although $\zeta_{k,l}$ is correlated with $t_{k,l}$ and $\phi_{k,l}$, it can be viewed as i.i.d. for all k and l after modulo-2π operation.

The decision variable of user 1 on the pth stream and the nth path of the MF is

$$Z_{p,n} = \int_{t_{1,n}}^{t_{1,n}+T} r(t)\alpha_{1,n}a_{1,p}(t-t_{1,n})\cos(\omega_0 t+\zeta_{1,n})dt \quad (7)$$

Assuming perfect channel estimation as in [2, 5], there is no influence on generality by setting $\phi_{1,l} = 0$ and $\tau_1 = 0$; hence, $\zeta_{1,l} = (\theta_1 - \omega_0 t_{1,l}) \bmod 2\pi$. For a bit sent from the transmitter, the decision variable at the RAKE receiver having the first λ paths locked can be represented as the sum of λ MF outputs. If the pth stream is intended, we obtain

$$\begin{aligned} Z|p &= \sum_{n=1}^{\lambda} Z_{p,n} \\ &= N_1 + D_1 + I_1 + I_2 + I_3 \end{aligned} \quad (8)$$

where N_1 is the noise due to $n(t)$, D_1 is the desired signal, I_1, I_2, and I_3 are the ISI (intersymbol interference) due to self (i.e. I_1, I_2) or other users' (i.e. I_3) streams. If $\lambda = L$, the RAKE receiver becomes a full-RAKE that locks the entire paths. Here, the signal to interference ratio (SIR) for the intended user is defined as [7]:

$$SIR = E[D_1]\{Var[N_1] + Var[I_1] + Var[I_2] + Var[I_3]\}^{-\frac{1}{2}} \quad (9)$$

As for the desired signal D_1, assume $b_{1,p}^{[0]}$ as the reference bit. Thus we have

$$D_1 = \sqrt{\frac{P}{2}}Tb_{1,p}^{[0]}\Gamma_1 \quad (10)$$

where $\Gamma_1 = \Sigma_{n=1}^{\lambda}\alpha_{1,n}^2$, is the sum of λ i.i.d. chi-squared random variables. And the variance of N_1 can easily be seen to be $Var[N_1] = (N_0T/4)\Sigma_{n=1}^{\lambda}\sigma_n^2$. In eqn. 8, the decision statistics $Z|p$ can be grouped into three different cases if we substitute eqns. 6 and 7 into eqn. 8 as follows:

(i) interference due to the remaining $L - 1$ paths, $(l \neq n)$ of the same stream of the same user 1: I_1;

(ii) interference due to the remaining $L - 1$ paths, $(l \neq n)$, from different streams, $(m \neq p)$, of the same user 1: I_2;

(iii) interference due to the L paths from arbitrary streams from other user $(k \neq 1)$: I_3.

3.1 Same stream interference I_1

In eqns. 1 and 2, owing to subcode concatenation, the intended stream of user 1 does not suffer from the self-user interference in the same path. Thus, I_1 and I_2 arise from the remaining $L - 1$ paths, $l \neq n$. Note that the interference experienced by the pth stream of user 1 can be expressed as

$$\begin{aligned} I_1 &= \sqrt{\frac{P}{2}}\sum_{n=1}^{\lambda}\sum_{l=1,l\neq n}^{L}\alpha_{1,l}\alpha_{1,n}\cos(\zeta_{1,l}-\zeta_{1,n}) \\ &\quad\times\int_{t_{1,n}}^{t_{1,n}+T} b_{1,p}(t-t_{1,l})a_{1,p}(t-t_{1,l})a_{1,p}(t-t_{1,n})dt \\ &= \sqrt{\frac{P}{2}}\sum_{n=1}^{\lambda}\left[\sum_{l=1,l\neq n}^{\lambda}h(n,l)+\sum_{l=\lambda+1}^{L}h(n,l)\right] \\ &= \sqrt{\frac{P}{2}}\left(I_{1,p}^{[1]}+I_{1,p}^{[2]}\right) \end{aligned} \quad (11)$$

where

$$h(n,l) = \alpha_{1,l}\alpha_{1,n}\cos(\zeta_{1,l}-\zeta_{1,n}) \times\int_{t_{1,n}}^{t_{1,n}+T} b_{1,p}(t-t_{1,l})a_{1,p}(t-t_{1,l})a_{1,p}(t-t_{1,n})dt \quad (12)$$

However, setting $l = 1$ and $n = 2$ or $l = 2$ and $n = 1$ in eqn. 12, we find that some terms are correlated (i.e. $\cos(\zeta_{1,l} - \zeta_{1,2}) = \cos(\zeta_{1,2} - \zeta_{1,l})$. Eqn. 11 can further be written as [7]:

$$\sum_{n=1}^{\lambda}\sum_{l=1,l\neq n}^{\lambda}h(n,l) = \sum_{n=1}^{\lambda-1}\sum_{l=n+1}^{\lambda}[h(n,l)+h(l,n)] \quad (13)$$

to split $h(n, l)$ into uncorrelated terms and utilise Gaussian approximation. From eqns. 11–13, one can write $I_{1,p}^{[1]}$ in terms of $R_p(t)$ as

$$\begin{aligned} I_{1,p}^{[1]} &= \sum_{n=1}^{\lambda-1}\sum_{l=n+1}^{\lambda}\alpha_{1,l}\alpha_{1,n}\cos(\zeta_{1,l}-\zeta_{1,n}) \\ &\quad\times\left[b_{1,p}^{[-1]}R_p(t_{1,l}-t_{1,n})+b_{1,p}^{[+1]}R_p(t_{1,l}-t_{1,n}) + 2b_{1,p}^{[0]}\hat{R}_p(t_{1,l}-t_{1,n})\right] \end{aligned} \quad (14)$$

where $b_{1,p}^{[-1]}$ and $b_{1,p}^{[+1]}$ represent the preceding and following bit of the reference bit $b_{1,p}^{[0]}$. And $R_p(t)$ and $\hat{R}_p(t)$ are continuous-time partial cross-correlation functions defined in [5] with subscript replaced by p. For simplicity, set $\delta_{1,n} = 0$, thus $t_{1,l} - t_{1,n} = (l-n)T_c + \delta_{1,l}$. Furthermore, we can regard $I_{1,p}^{[1]}$ as a stationary random process with zero mean. The variance of $I_{1,p}^{[1]}$ can be derived as

$$Var\left[I_{1,p}^{[1]}\right] = \frac{T_c^2}{3}\sum_{n=1}^{\lambda-1}\sum_{l=n+1}^{\lambda}\sigma_l^2\sigma_n^2[A_1(l-n)+A_2(l-n)] \quad (15)$$

by performing time average over $b_{1,p}^{[-1]}$, $b_{1,p}^{[0]}$, $b_{1,p}^{[+1]}$, and $R_p(t_{1,l} - t_{1,n})$. These variables are slowly varying and independently distributed time functions. It is adequate to make the above assumption [5, 7]. $A_1(l-n)$ and $A_2(l-n)$ are real functions defined in [7]. Besides, σ_l^2 is defined as $Var[\alpha_{1,l}] = \sigma_l^2$. With similar mathematical manipulations, the variance of $I_{1,p}^{[2]}$ can be expressed as:

$$Var\left[I_{1,p}^{[2]}\right] = \frac{T_c^2}{6}\sum_{n=1}^{\lambda}\sum_{l=\lambda+1}^{L}\sigma_l^2\sigma_n^2A_1(l-n) \quad (16)$$

From eqns. 11, 15 and 16, the variance of I_1 can be expressed as the sum of $Var[I_{1,p}^{[1]}]$ and $Var[I_{1,p}^{[2]}]$ as follows:

$$Var[I_1] = \frac{PT_c^2}{12}\left[\sum_{n=1}^{\lambda}\sum_{l=1,l\neq n}^{L}\sigma_l^2\sigma_n^2A_1(|l-n|) + 2\sum_{n=1}^{\lambda-1}\sum_{l=n+1}^{\lambda}\sigma_l^2\sigma_n^2A_2(l-n)\right] \quad (17)$$

In eqn. 17, the second term of the right-hand side (RHS) is zero if we set $\lambda = 1$; namely, it can be viewed as the correlation interference between the fingers of the RAKE receiver. However, the first term of the RHS is associated with the correlation interference among all the paths.

3.2 Other streams interference I_2

From eqn. 7, I_2 can be represented as

$$I_2 = \sqrt{\frac{P}{2}} \sum_{n=1}^{\lambda} \sum_{\substack{m=1 \\ m\neq p}}^{M_1} \sum_{\substack{l=1 \\ l\neq n}}^{L} \alpha_{1,l}\alpha_{1,n} \cos(\zeta_{1,l} - \zeta_{1,n}) \times \int_{t_{1,n}}^{t_{1,n}+T} b_{1,p}(t - t_{1,l}) a_{1,p}(t - t_{1,l}) a_{1,m}(t - t_{1,n}) dt \tag{18}$$

To simplify eqn. 18, the following formula is utilised [7]:

$$\int_0^T b(t - \tau^{[*]}) a_{p^*}(t - \tau^*) a_{m^*}(t) dt = \left\{ b^{[*]}[C_{p^*,m^*}(f + 1 - N) - C_{p^*,m^*}(f)] + b^{[0]}[C_{p^*,m^*}(f + 1) - C_{p^*,m^*}(f)] \right\} \delta \tag{19}$$

with $m^* = m$, $p^* = p$, $\tau^* = t_{1,l} - t_{1,n}$, $f = \lfloor |\tau^*|/T_c \rfloor = |l - n|$, $\delta = |\tau^* - fT_c| = (\delta_{1,l} - \delta_{1,n}) \bmod T_c$ which is uniformly distributed on $[0, T_c)$. Substitute eqn. 19 into eqn. 18 and perform derivations similar to $Var[I_1]$, the variance of I_2 is

$$Var[I_2] = \frac{PT_c^2}{12} \sum_{n=1}^{\lambda} \sum_{m=1, m\neq p}^{M_1} \sum_{l=1, l\neq n}^{L} \sigma_l^2 \sigma_n^2 A_3(|l - n|) \tag{20}$$

where $A_3(|l - n|)$ is defined in [7] with subscripts replaced by m^* and p^*.

3.3 Other user interference I_3

I_3 can be regarded as the sum of the interference of the λ RAKE fingers, that is

$$I_3 = \sqrt{\frac{P}{2}} \sum_{n=1}^{\lambda} I_{3,p,n} \tag{21}$$

From eqns. 6–8, $I_{3,p,n}$ takes the form:

$$I_{3,p,n} = \sum_{k=2}^{K} \sum_{m=1}^{M_k} \sum_{l=1}^{L} \alpha_{k,l}\alpha_{1,n} \cos(\zeta_{k,l} - \zeta_{1,n}) \times \int_{t_{1,n}}^{t_{1,n}+T} b_{k,m}(t - \tau_k - t_{k,l}) \times a_{k,m}(t - \tau_k - t_{k,l}) a_{1,p}(t - t_{1,n}) dt \tag{22}$$

Utilising change of variables in the integral and regarding $(\tau_k + t_{k,l}) \bmod T$ as a uniformly distributed r.v. on $[0, T)$, the variance of I_3 becomes

$$Var[I_3] = \frac{PT_c^2}{12N} \sum_{k=2}^{K} \sum_{n=1}^{\lambda} \sum_{m=1}^{M_k} \sum_{l=1}^{L} r_{(k-1)\hat{M}+m,p} \sigma_l^2 \sigma_n^2 \tag{23}$$

where $r_{(k-1)\hat{M}+m,p}$ is defined in [5] with subscript replaced by $(k - 1)\hat{M} + m$ and p. Notice that, in a synchronous MC-CDMA system where $\tau_k = 0$ and $L = 1$, $Var[I_3]$ vanishes if all the users are with a nonoverlapping Hadamard–Walsh row index.

Finally, combining eqns. 8, 10, 17, 20 and 23, the variance of $Z|p$ is given by

$$Var[Z|p] = \frac{N_0 T\lambda}{4} + \frac{PT_c^2}{12}\xi_1 + \frac{PT_c^2}{12}\xi_2 + \frac{PT_c^2}{12}\xi_3 \tag{24}$$

where

$$\xi_1 = \sum_{n=1}^{\lambda} \sum_{l=1, l\neq n}^{L} \sigma_l^2 \sigma_n^2 A_1(|l - n|) + 2 \sum_{n=1}^{\lambda-1} \sum_{l=n+1}^{\lambda} \sigma_l^2 \sigma_n^2 A_2(l - n)$$

$$\xi_2 = \sum_{n=1}^{\lambda} \sum_{m=1, m\neq p}^{M_1} \sum_{l=1, l\neq n}^{L} \sigma_l^2 \sigma_n^2 A_3(|l - n|)$$

$$\xi_3 = \sum_{k=2}^{K} \sum_{n=1}^{\lambda} \sum_{m=1}^{M_k} \sum_{l=1}^{L} r_{(k-1)\hat{M}+m,p} \sigma_l^2 \sigma_n^2$$

3.4 Bit error rate analysis

The performance of a MC system can be judged by SIR and BER (bit error rate). It is assumed that BPSK (binary phase shift keying) modulation is used in this discussion. Substituting eqn. 24, and $Var[N_1]$ into eqn. 9, the instantaneous SIR per bit becomes

$$SIR = \frac{\sqrt{\frac{PT^2}{2}}\Gamma_1}{\sqrt{\frac{N_0 T\lambda}{4} + \frac{PT_c^2}{12}\xi_1 + \frac{PT_c^2}{12}\xi_2 + \frac{PT_c^2}{12\hat{N}}\xi_3}} \tag{25}$$

$$= U\Gamma_1 \tag{26}$$

where

$$U = \left(\frac{N_0\lambda}{2PT} + \frac{1}{6N^2}\xi_1 + \frac{1}{6N^2}\xi_2 + \frac{1}{6N^3}\xi_3 \right)^{-\frac{1}{2}} \tag{27}$$

In obtaining the average bit error rate P_e, conditional integral based on the channel fading distribution should be calculated as

$$P_e = \int_0^{\infty} Q\left(\sqrt{2U\Gamma_1}\right) p(U\Gamma_1) d(U\Gamma_1) \tag{28}$$

where $Q(\sqrt{(2U\Gamma_1)})$ is the instantaneous bit error probability for BPSK modulation, and $p(U\Gamma_1)$ is the density function of chi-squared distribution with 2λ degrees of freedom. After some mathematical manipulations [4, 17],

$$P_e = \left(\frac{1}{2}\right)^{\lambda} \left(1 - \sqrt{\frac{\chi}{1+\chi}}\right)^{\lambda} \times \left[\sum_{k=1}^{\lambda-1} \binom{\lambda + k - 1}{k} \left(\frac{1}{2}\right)^k \left(1 + \sqrt{\frac{\chi}{1+\chi}}\right)^k \right] \tag{29}$$

where $\chi = U(\sigma_l^2)^{-1}$.

4 Numerical results and discussion

As mentioned in Section 3.4, the bit error rate of each stream depends on the cross-correlation of concatenated sequences. Borth and Pursley [6] prove that the performance of random codes lies between the best and the worst choice of codes in a frequency selective fading channel. However, it is not the objective of this paper to find the best code of MC-CDMA. Thus, it is adequate to adopt

random codes as primary codes, which are computer generated using the C library. Notice that the primary code of each user is randomly assigned by the computer. The number of users in this system is assumed to be ten, and nine of them are the interferers with respect to the intended receiver.

Fig. 4 shows the BER against SNR when different number of concatenated subcodes are used in an AWGN channel. In this example, each user has the same total power, regardless of the number of subcodes it is using. The approximate formula in eqn. 1 of [12] is drawn here for $N = 64$ and 128 in lines 1 and 6, respectively, regardless of the number of subcodes that are used. Examine the case $N = 64$, the curve corresponding to 4 subcodes ($M_k = 4$) shows the worst performance among the five curves drawn for $N = 64$. A similar phenomenon exists in the five curves drawn for $N = 128$. The deviation among the curves in each of the two sets says that the cross-correlation property among them has an impact on system performance. That is, a stream with relatively better codes, or alternatively, lower cross-correlation, achieves lower BER. Our analysis produces results more precise than eqn. 1 of [12]. Compared with the approximate analysis developed in [12], our improved approach produces more refined and more accurate results.

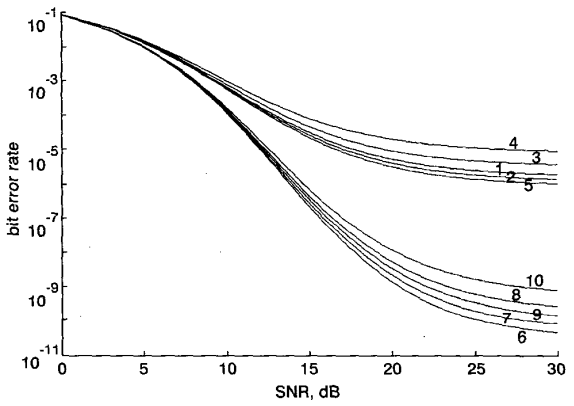

Fig. 4 *MC-CDMA in AWGN channel with exact and approximate results*
Curve 1: $N = 64$ (approximate); curve 2: $N = 64$, $M_k = 1$ (improved); curve 3: $N = 64$, $M_k = 2$ (improved); curve 4: $N = 64$, $M_k = 4$ (improved); curve 5: $N = 64$, $M_k = 8$ (improved); curve 6: $N = 128$ (approximate); curve 7: $N = 128$, $M_k = 1$ (improved); curve 8: $N = 128$, $M_k = 2$ (improved); curve 9: $N = 128$, $M_k = 4$ (improved); curve 10: $N = 128$, $M_k = 8$ (improved)

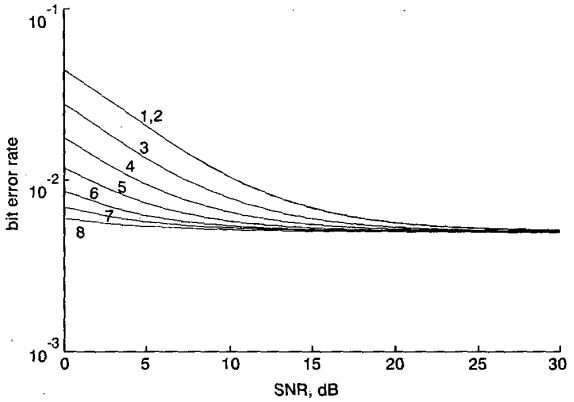

Fig. 5 *Conventional CDMA against MC-CDMA in multipath fading channel with $L = 4$, $\lambda = 3$*
Curve 1: conventional CDMA; curve 2: MC-CDMA, $M_k = 1$; curve 3: MC-CDMA, $M_k = 2$; curve 4: MC-CDMA, $M_k = 4$; curve 5: MC-CDMA, $M_k = 8$; curve 6: MC-CDMA, $M_k = 16$; curve 7: MC-CDMA, $M_k = 32$; curve 8: MC-CDMA, $M_k = 64$

In contrast to Fig. 4, Fig. 5 considers equal user rate, equal user power, equal bandwidth, and a multipath fading channel with $L = 4$ and $\lambda = 3$, which means that the RAKE receiver can lock three out of the four paths. Unless otherwise mentioned, the spread spectrum processing gain is set to 64 for $M_k = 1$ and all users are with homogeneous traffic rates. After serial-to-parallel conversion, the power and rate of each stream are divided by M_k from those of the sending user. Each parallel stream is further spread to the entire bandwidth allocated. For example, the SS processing gain of $M_k = 2$ and $M_k = 4$ are 128 and 256, respectively. The performance of the MC system improves as the number of streams increased. The conventional CDMA with RAKE receiver is also shown. For $M_k = 1$, the performance of the MC system is slightly better than the conventional RAKE due to subcode concatenation. As demonstrated in Fig. 5, all results surpass that of the conventional CDMA. At higher SNR, however, the BER for larger M_k approaches the conventional CDMA due to an equally assigned frequency band.

Figs. 6 and 7 present the BER against SNR with double bandwidth and one more multipath than Fig. 5, respectively. In Fig. 6, all curves are vertically shifted downward due to trading more bandwidth for combating multipath fading. Fig. 7 shows the performance of $L = 5$, $\lambda = 3$. The extra path that is not locked by the RAKE receiver deteriorates the system performance.

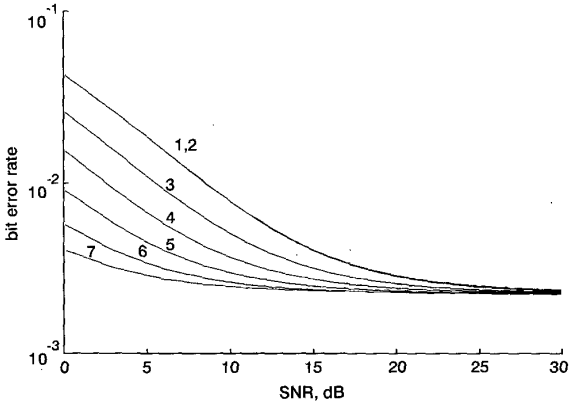

Fig. 6 *Conventional CDMA against MC-CDMA in multipath fading channel with double bandwidth*
Curve 1: conventional CDMA; curve 2: MC-CDMA, $M_k = 1$; curve 3: MC-CDMA, $M_k = 2$; curve 4: MC-CDMA, $M_k = 4$; curve 5: MC-CDMA, $M_k = 8$; curve 6: MC-CDMA, $M_k = 16$; curve 7: MC-CDMA, $M_k = 32$

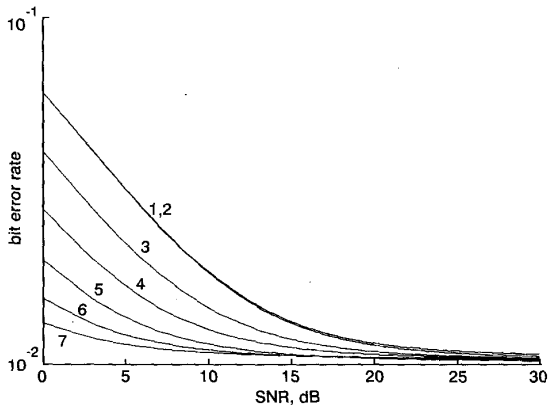

Fig. 7 *Conventional CDMA against MC-CDMA in multipath fading channel with $L = 5$, $\lambda = 3$*
Curve 1: conventional CDMA; curve 2: MC-CDMA, $M_k = 1$; curve 3: MC-CDMA $M_k = 2$; curve 4: MC-CDMA, $M_k = 4$; curve 5: MC-CDMA, $M_k = 8$; curve 6: MC-CDMA, $M_k = 16$; curve 7: MC-CDMA, $M_k = 32$

5 Conclusions

In this paper, a simplified MC-CDMA model with properly selected concatenation subcodes is analysed rigorously. With this arrangement, an M_k-rate user is serial-to-parallel converted to M_k mutually orthogonal streams, which further modulates the radio carrier to the same frequency band. The self-user interference on the same path vanishes and the spectral efficiency is increased due to the concatenated subcodes. Besides, path diversity is achievable with a RAKE receiver at the receiving side. Of particular interest, the performance of the transmitter/receiver pairs in an urban environment (no direct path) is investigated. The numerical results reveal that the MC-CDMA excels the conventional arrangement when the SNR is low and shows comparable performance at high SNR. Furthermore, considerable variation is seen in eqn. 1 of [12] when compared with ours in an AWGN channel.

In the reverse link, a major problem of MC-CDMA and other popular techniques (e.g. multicarrier CDMA), is the nonconstant envelope of the transmitted signal. In this paper, the effect of nonconstant envelope on the performance due to (e.g. amplifier nonlinearity), is not addressed. This is a topic for further research. In addition, powerful source-channel coding with burst error correction capability, especially suitable in high speed multimedia transmission is desired to further improve the system performance.

6 Acknowledgments

The authors thank the anonymous referees for helpful suggestions. In particular, the authors thank one referee for pointing out that the autocorrelation properties of the spreading codes have an impact on the transmission performance which depends on the power delay profile of the channel, and only for idealised 'random' codes this impact can be neglected.

7 References

1 I, C.L., and GITLIN, R.D.: 'Multi-code CDMA wireless personal communications networks'. Proceedings of IEEE ICC'95, Seattle, 1995, pp. 1060–1064
2 LIU, Z., KAROL, M.J., ZATKI, M.E., and ENG, K.Y.: 'A demand-assignment access control for multi-code DS-CDMA wireless packet (ATM) networks'. Proceedings of IEEE INFO-COM'96, San Francisco, 1996, pp. 713–721
3 I, C.L., POLLINI, G.P., OZAROW, L., and GITLIN, R.D.: 'Performance of multi-code CDMA wireless personal communications networks'. Proceedings of IEEE VTC'95, Chicago, 1995, pp. 907–911
4 PROAKIS, J.A.: 'Digital communications' (McGraw-Hill, New York, 1995, 3rd edn.)
5 PURSLEY, M.: 'Performance evaluation for phase-coded spread-spectrum multiple access communications. Part I: System analysis', *IEEE Trans. Commun.*, 1977, **COM–25**, (8), pp. 795–799
6 BORTH, D.E., and PURSLEY, M.: 'Analysis of direct sequence spread spectrum multiple access communication over Rician fading channels', *IEEE Trans. Commun.*, 1979, **COM–27**, (10), pp. 1566–1577
7 SOUROUR, E.A., and NAKAGAWA, M.: 'Performance of orthogonal multicarrier CDMA in a multipath fading channel', *IEEE Trans. Commun.*, 1996, **44**, (3), pp. 356–367
8 PARK, S.Y., YUN, S.B., and KANG, C.G.: 'Performance of multi-carrier parallel combinatory DS-CDMA system', *IEICE Trans. Commun.*, 1998, **E81–B**, (9), pp. 1758–1769
9 SANADA, Y., and ARAKI, K.: 'A variable length code transmission technique on multi-code DS/SS systems', *IEICE Trans. Commun.*, 1998, **E81–B**, (3), pp. 625–636
10 SCHOTTEN, H.D., BOLL, H.E., and BUSHOOM, A.: 'Adaptive multi-rate multi-code CDMA systems'. Proceedings of IEEE VTC'98, Ottawa, 1998, pp. 782–785
11 SCHOTTEN, H.D., BOLL, H., and BUSHOOM, A.: 'Multi-code CDMA with variable sequence-sets'. Proceedings of IEEE ICUPC'97, San Diego, 1997, pp. 628–631
12 LEE, S.J., LEE, H.W., and SUNG, D.K.: 'Capacity calculation in DS-CDMA systems supporting multi-class services'. Proceedings of IEEE PIMRC'97, San Diego, 1997, pp. 297–301
13 LIU, Z., KAROL, M.J., ZARKI, M.E., and ENG, K.Y.: 'Interference issues in multi-code CDMA networks'. Proceedings of IEEE PIMRC'96, Taipei, 1996, pp. 98–102
14 LIU, Z., KAROL, M.J., ZARKI, M.E., and ENG, K.Y.: 'Channel access and interference issues in multi-code DS-CDMA wireless packet (ATM) networks', *Wirel. Netw.*, 1996, pp. 173–193
15 OHNO, K., SAWAHASHI, M., and ADACHI, F.: 'Wideband coherent DS-CDMA'. Proceedings of IEEE VTC'95, Chicago, 1995, pp. 779–783
16 WILHELMSSON, L., and ZIGANGIROV, K.S.: 'Analysis of MFSK frequency-hopped spread-spectrum multiple-access over a Rayleigh fading channel', *IEEE Trans. Commun.*, 1998, **46**, (10), pp. 1271–1274
17 PETERSON, R.L., ZIEMER, R.E., and BORTH, D.E.: 'Introduction to spread spectrum communications' (Prentice-Hall, New York, 1995, 1st edn.)